2021 43rd Annual International Conference of the
IEEE Engineering in Medicine & Biology Society (EMBC)
Oct 31 - Nov 4, 2021. Virtual Conference

An Integrated Method for Large Deformable Registration of Brain Images

Pengcheng Yu and Yao Li*, *Senior Member, IEEE*

***Abstract*— Large deformable registration of brain images is essential for a variety of clinical imaging applications. State-of-the-art diffeomorphic registration methods, such as large deformation diffeomorphic mapping (LDDMM), have high computational complexity and often require pre-processing to account for large, global displacements or rotations. In this paper, we present an integrated method that fuses landmark-based thin-plate splines (TPS), patch-based B-spline and partial differential equation (PDE) based registrations synergistically to achieve improved accuracy and efficiency for large deformable registration of brain image. Landmark-based TPS and patch-based B-spline were used for global affine transformation followed by deformable registration using LDDMM. The anatomical discrepancies between the source and target images were significantly reduced after TPS and B-spline based registration. As a result, the PDE based deformable registration could be done efficiently and effectively. The performance of the proposed method has been evaluated using simulation and real human brain image data, which provided more accurate registration than spline or PDE-based methods. Moreover, the computational efficiency of our method was significantly better than PDE-based methods. The proposed method may be useful for handling large deformable registration of brain images in various brain imaging applications.**

I. Introduction

Large deformable registration of brain images is an essential step in various longitudinal and population brain imaging studies. Some examples include registration of pathological brain images to a normal brain atlas [1, 2], quantitative analysis of infant brain development and study of the aging brain [3, 4]. Human neuroanatomies vary in both global shapes and local structures across a population. For large deformable registration of brain images, the key is to efficiently identify a diffeomorphic deformation field that will achieve accurate alignment of the corresponding neuroanatomical features of different brain images.

Large deformation diffeomorphic mapping (LDDMM) is one of the key diffeomorphic registration methods in practical use, which models spatial deformation by time integration of a sufficiently regular velocity field [5-8]. The method finds a velocity field $\boldsymbol{v}$ such that the mismatch between the source image and the target image is minimized subject to a smoothness regularization. The deformation filed $\boldsymbol{\emptyset}$ is modelled by a partial differential equation (PDE) that allows large diffeomorphic deformable transformation. To ensure numerical stability, the method requires the size of the time step to be sufficiently small. Besides, the integration of the velocity field has high computational complexity. Therefore, LDDMM is computationally inefficient for many practical applications. Several methods have been proposed to address this problem by using, for example, a stationary velocity field to reduce the degrees of freedom of the deformation model [5, 8]. Another problem with LDDMM is that the estimated initial momentum may not accurately encode the final diffeomorphism, especially when large deformation is required. Due to the regularization effect, it needs good pre-processing to account for large, global displacements or rotations. To address this problem, the overall deformation field f_s is often decomposed into two parts, i.e., $f_s(x) = f_{se}(x) + f_{sr}(x)$, where $f_{se}(x)$ is the predicted initial deformation field and $f_{sr}(x)$ is the remaining part. In the previous studies, $f_{se}(x)$ were estimated using learning-based methods [9, 10], but the local deformation may not be accurately determined because of the use of global model to represent the entire deformation field.

We present here an integrated method that fuses landmark based thin-plate splines (TPS), patch-based B-spline and PDE based registration synergistically to achieve improved accuracy and efficiency for large deformable registration of brain images. Landmark-based TPS registration has been widely used for large global deformation using affine transformation [11]. It is especially useful for compensating large anatomical discrepancies between paired images and establishing local/patch correspondence between images. On the other hand, B-spline based Free-Form Deformations (FFD) [12] is efficient for determining local deformations. FFD is characterized by smooth, locally controlled, and fast interpolation, and could be implemented using a hierarchical multi-resolution structure. Perhaps more importantly, the basis functions of a cubic B-spline have a limited support, which is desirable for modeling subtle local patch-wise deformations [13].

In our proposed method, we use landmark-based TPS and patch-based B-spline to determine an initial displacement field for LDDMM. We then use LDDMM to further improve the deformation transformation by using a PDE model to pick subtle local deformations. The performance of our proposed method has been evaluated using simulation and real human brain image data. Our experimental results indicate that the proposed method could improve: 1) registration accuracy

This research was supported by National Natural Science Foundation of China (No. 81871083) and Shanghai Jiao Tong University Scientific and Technological Innovation Funds (2019QYA12).

Pengcheng Yu and Yao Li (Tel: +86-21-62932981; e-mail: yaoli@sjtu.edu.cn) are with School of Biomedical Engineering, Shanghai Jiao Tong University, Shanghai, 200030, P. R. China.

over spline based registration, and 2) efficiency and accuracy over direct PDE-based registration. Details of the proposed method are given in Section 2, which is followed by experimental results in Section 3 and the paper conclusions in Section 4.

II. METHOD

Considering a target image $\boldsymbol{F}$ and a source image $\boldsymbol{M}$, deformable registration between the image pair ($\boldsymbol{F}$, $\boldsymbol{M}$) can be formally defined as follows:

$$\hat{\boldsymbol{u}} = \underset{\boldsymbol{u} \in \boldsymbol{U}}{\operatorname{argmax}} \boldsymbol{SIM}\big(\boldsymbol{F}, \boldsymbol{M}(\boldsymbol{u})\big). \tag{1}$$

The objective is to find an optimal displacement field $\hat{\mathbf{u}}$ from all the possible displacement fields $\mathbf{U}$ such that the alignment accuracy between $\mathbf{M}$ and $\mathbf{F}$ is maximized. In order to reduce the computational complexity of direct registration, we decomposed the overall displacement field into three parts, i.e.,

$$\hat{\boldsymbol{u}} = \hat{\boldsymbol{u}}_{TPS} + \hat{\boldsymbol{u}}_{B\text{-}Spline} + \hat{\boldsymbol{u}}_{PDE}. \tag{2}$$

where $\hat{\boldsymbol{u}}_{TPS}$ is the predicted initial global large displacement field using TPS, $\hat{\boldsymbol{u}}_{B\text{-}Spline}$ is the local displacement field estimated using patch-based B-spline, and $\hat{\boldsymbol{u}}_{PDE}$ represents the remaining displacement field measured by PDE-based registration.

A. Landmark-based TPS registration

Landmark-based TPS registration method defines a transformation matrix between source and target images through the matching of the corresponding landmarks. The deformation model can be expressed as [11]:

$$\mathbf{T_t}(x, y, z) = a_1 + a_2 x + a_3 y + a_4 z + \sum_{j=1}^{n} c_j \boldsymbol{U}\left(\left(x_j, y_j, z_j\right) - (x, y, z)\right). \tag{3}$$

where $\boldsymbol{U}(x, y, z) = \sqrt{x^2 + y^2 + z^2}$ is radial basis function of thin-plate splines and c_j is the j-th coefficient corresponding to the j-th landmark. The displacement field predicted by TPS can be expressed as:

$$\hat{\boldsymbol{u}}_{TPS} = \mathbf{T_t}(x, y, z) - (x, y, z). \tag{4}$$

In this method, identification of the corresponding landmarks is critical in order to minimize the bending energy of splines and ensure smooth deformation. In our work, the corresponding landmarks in the source image were identified by applying an initial B-spline registration field to landmarks defined in the image using scale-invariant feature transform (SIFT) [14]. After the corresponding landmark pairs were established, the large global deformation between the source and target images were determined using TPS deformation model.

B. Patch-based B-spline registration

The above TPS registration works well for global deformation but lacks the local deformation capability. B-spline registration is suitable for recovering local subtle deformation and is computationally efficient even with a large number of control nodes. The B-spline transformation function is defined as [12]:

$$\mathbf{T_b}(x, y, z) = \sum_{l=0}^{3} \sum_{m=0}^{3} \sum_{n=0}^{3} B_l(u) B_m(v) B_n(w) \boldsymbol{\Phi}_{i+l, j+m, k+n}. \tag{5}$$

where $\boldsymbol{\Phi}$ denotes an $n_x \times n_y \times n_z$ mesh of control points $\boldsymbol{\Phi}_{i, j, k}$ with uniform spacing. Functions B_0 through B_3 are basis functions of cubic B-spline and are defined as follows:

$$\begin{aligned} B_0(r) &= (-r^3 + 3r^2 - 3r + 1) / 6, \\ B_1(r) &= (3r^3 - 6r^2 + 4) / 6, \\ B_2(r) &= (-3r^3 + 3r^2 + 3r + 1) / 6, \\ B_3(r) &= r^3 / 6. \end{aligned} \tag{6}$$

where $0 \le r < 1$.

A hierarchical multiresolution implementation of the B-spline model provides an even more efficient solution, with $\Phi^1, \ldots, \Phi^S$ denote a hierarchy of uniform grids at different resolutions. Each grid Φ^s defines a local deformation at the associated level of resolution. With this, the local transformation could be written as:

$$\mathbf{T_b}(x, y, z) = \sum_{s=1}^{S} \mathbf{T_b^s}(x, y, z). \tag{7}$$

The displacement field estimated by patch based B-spline can be derived as:

$$\hat{\boldsymbol{u}}_{B\text{-}Spline} = \mathbf{T_b}(x, y, z) - (x, y, z). \tag{8}$$

In order to ensure that the transformation is diffeomorphic, we constrained the Jacobian determinant of the registration field to be positive, and added isotropic total variation spatial regularization [15] on the displacement field. The registration was performed in a patch-wise way, allowing more flexible transformation in local areas. In our implementation, a patch size of 128 × 128 × 128 and a sliding window at step length of 100 were applied. In each patch volume, the displacement $\boldsymbol{u}(\boldsymbol{x})$ for a given point $\boldsymbol{x}$ in the image was interpolated from the neighboring control points by the respective basis functions and normalized using cross correlation (NCC) as similarity measurements.

C. PDE-based registration

The PDE-based model operates directly on the velocity field $\boldsymbol{v}$, which constrains the neighboring voxels to deform similarly and ensures spatially smooth velocity field within small time intervals. Given this, the final large deformation is achieved through integration of velocity over time. A well-known viscous fluid model governed by the Navier-Stokes PDE is defined as [6]:

$$\mu_f \nabla^2 \boldsymbol{v} + \left(\mu_f + \lambda_f\right) \nabla(\nabla \cdot \boldsymbol{v}) + \boldsymbol{b} = 0. \tag{9}$$

where μ and λ are the viscosity constants, $\nabla^2 = \nabla^T \nabla$ is the Laplacian operator and $\boldsymbol{b}$ is the body force that drives the registration based on an image matching criterion. Based on the model of viscous fluids, the remaining diffeomorphic transformation was derived as an integration of time-dependent velocity field as:

$$\hat{\boldsymbol{u}}_{PDE} = \boldsymbol{\Phi}_1 = \boldsymbol{\Phi}_0 + \int_0^1 \boldsymbol{v}_t(\boldsymbol{\Phi}_t)\, dt. \tag{10}$$

A path was given for $\emptyset_t : \Omega \rightarrow \Omega$, $t \in [0,1]$, which started with the identity mapping at $t = 0$ and terminated at $t = 1$. This formulation of the flow ensured the transformation to be invertible and continuously differentiable. To ensure the smoothness of deformation, the velocity fields were regularized using an appropriate differential operator [7]. The optimal transformation was then defined by the sequence of velocity fields that minimize the energy function:

$$\hat{\boldsymbol{v}}_t = \underset{\boldsymbol{v}:\, \dot{\emptyset}_t = \boldsymbol{v}_t(\emptyset_t)}{\operatorname{argmin}} \left(\int_0^1 \int_\Omega \|\boldsymbol{L}\boldsymbol{v}\|^2 + \frac{1}{\sigma^2} \left\| I_0 \circ \emptyset_1^{-1} - I_1 \right\|^2 \right). \quad (11)$$

where I_0 denotes the source image and I_1 represents the target image.

III. Results and Discussion

We evaluated the performance of our method through experiments with both simulated and real human brain images. For comparison, the direct PDE-based method was implemented using the Diffeomorphic Anatomical Registration Through Exponential Lie algebra (DARTEL) [5]. The TPS alone and TPS combined with patch-based B-spline registration methods were also implemented for performance comparison.

In the simulation experiments, we first performed a large deformation for a typical disk to "C" task. Where large deformation exists in this experiment. As shown in Fig. 1(a), the spline based methods such as TPS or TPS+B-spline could not handle such large deformations for its limit model performance. Second, we choose a toy example where large global affine transformation exists, for which the direct PDE-based method could not handle the affine transformation well, as seen in Fig. 1(b). In comparison, our proposed method showed robust and satisfactory deformation performance for both cases.

Next, we compared the performance of our proposed method for real brain MRI images. For comparison, we used the state-of-the-art methods including diffeomorphic Demons (D. Demons) [16] and symmetric normalization (SyN) in the Advanced Normalized Tools (ANTs) software package [17]. Deformable registration was conducted between healthy brain image pairs (100 pairs) and brain image pairs from Alzheimer's disease (AD) patients (90 pairs) with severe atrophy. The healthy brain T1-weighted images were obtained from the Human Connectome Project (HCP) database (http://www.humanconnectomeproject.org/). The AD patient brain T1-weighted images were obtained from the Alzheimer's Disease Neuroimaging Initiative (ADNI) database (http://adni.loni.usc.edu/).

The results are shown in Fig. 2 and Fig. 3. For a better illustration of the performance, the white matter (WM), gray matter (GM), pallidum, putamen and hippocampus were segmented from the T1-weighted images for tissue-level registrations. As can be seen, the results obtained using our integrated method were better in deforming the structural details compared with the other methods. The quantitative evaluation and comparison of the deformation performance are shown in Table I. From the dice similarity coefficient (DSC) comparison, our proposed method outperformed the others for both HCP data and AD data. For example, the DSC of our proposed method in HCP data were 0.8802 for GM and 0.8763 for WM, which were higher than direct PDE (GM: 0.8623; WM: 0.8495), D. Demons (GM: 0.8576; WM: 0.8407) and SyN (GM: 0.8773; WM: 0.8501) methods. Moreover, the proposed method can achieve more accurate registration results in brain subcortical regions such as pallidum, putamen and hippocampus, as shown in Table I. With TPS firstly as a pre-registration step to account for large, global displacements or rotations and following local patch based B-spline for local large deformations, PDE based method can converge more accurately and quickly. To evaluation the computation efficiency, the above algorithms were tested in CPU (Intel Core i5-8250U). The overall running time of our proposed method was 45 minutes, which was significantly less than direct PDE method, which took 82 minutes.

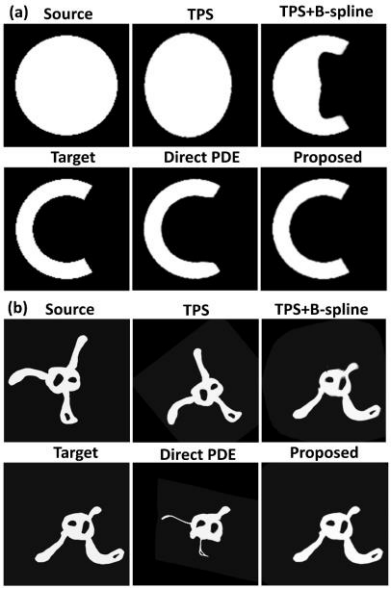

Figure 1: Comparison of registration performance of TPS, TPS+B-spline, Direct PDE and our integrated method for (a) a large deformation disk to "C" task; (b) a large global affine transformation task. Our integrated method achieved the best deformation performance compared to the others.

TABLE I. Quantitative comparison results for human brain images deformations. The direct PDE, D.Demons and SyN methods were compared with our integrated approach in both HCP and ADNI datasets .

	DSC (GM)		DSC (WM)		DSC (Pallidum)		DSC (Putamen)		DSC (Hippocampus)		DSC (minute)	
Methods	HCP	ADNI	HCP	ADNI	HCP	ADNI	HCP	ADNI	HCP	ADNI	HCP	ADNI
Direct PDE	0.8623	0.7859	0.8495	0.8358	0.7642	0.7525	0.7734	0.7645	0.7702	0.7610	82	75
D. Demons	0.8576	07801	0.8407	0.8295	0.7426	0.7387	0.7624	0.7433	0.7643	0.7533	14	11
SyN	0.8773	0.7942	0.8501	0.8408	0.7891	0.7787	0.7803	0.7887	0.8035	0.7895	47	44
Proposed	0.8802	0.8355	0.8763	0.8672	0.8103	0.7998	0.8021	0.8073	0.8223	0.8016	45	43

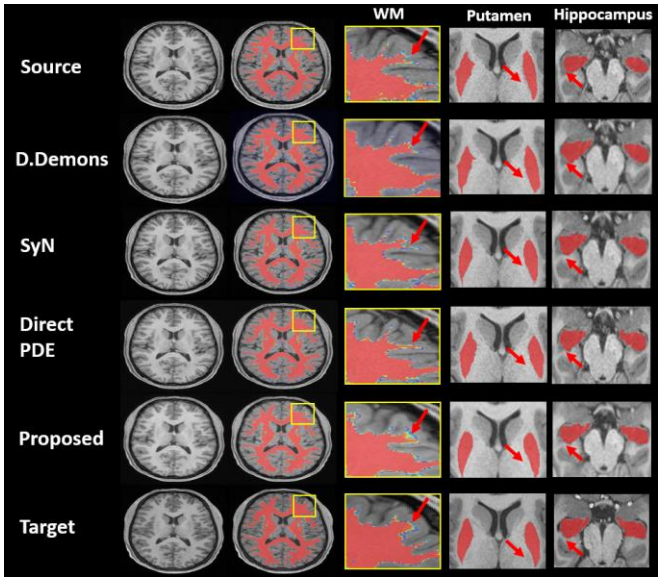

Figure 2: Comparisons of registration performance for real human brain images using HCP dataset. From top to down: transformation of a single slice of source image to the target image using D. Demons, SyN, Direct PDE, and the proposed method, respectively. The last three columns are zoom-in images of white matter, putamen and hippocampus. Inside the yellow boxes: local white matter regions.

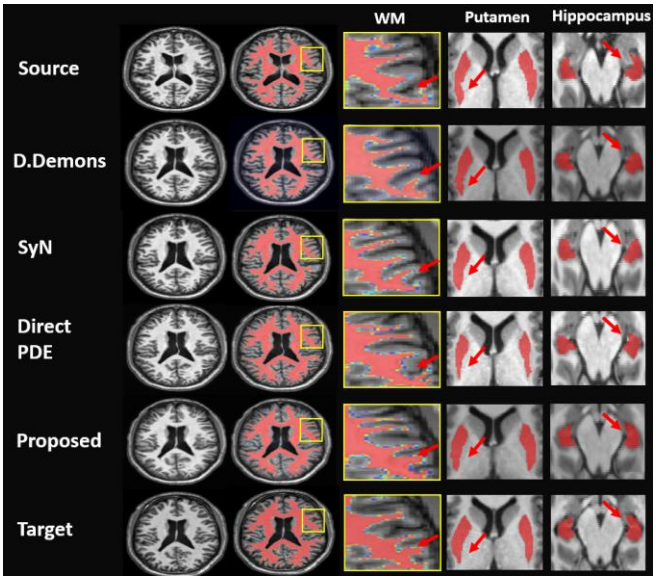

Figure 3: Comparisons of registration performance for AD patients brain images using ADNI dataset. From top to down: transformation of a single slice of source image to the target image using D. Demons, SyN, Direct PDE, and the proposed method, respectively. The last three columns are zoom-in images of white matter, putamen and hippocampus. Inside the yellow boxes: local white matter regions.

IV. Conclusion

In this paper, we proposed a novel method for large deformable registration of brain images by effectively integrating landmark-based TPS, patch-based B-spline, and PDE-based registration. The performance of the proposed method has been evaluated using simulations and real human brain image data. Our proposed method demonstrated higher accuracy than the state-of-the-art spline, D. Demons or PDE-based methods. Moreover, the computational efficiency of our method was better than PDE-based method. The proposed method can be useful for handling large deformable registration of brain images in various brain imaging applications.

References

[1] A. Mohamed, E. I. Zacharaki, D. Shen, and C. Davatzikos, "Deformable registration of brain tumor images via a statistical model of tumor-induced deformation," *Med Image Anal,* vol. 10, no. 5, pp. 752-63, Oct, 2006.

[2] E. I. Zacharaki, D. Shen, S. K. Lee, and C. Davatzikos, "ORBIT: a multiresolution framework for deformable registration of brain tumor images," *IEEE Trans Med Imaging,* vol. 27, no. 8, pp. 1003-17, Aug, 2008.

[3] S. Ahmad, Z. Wu, G. Li, L. Wang, W. Lin, P. T. Yap, and D. Shen, "Surface-constrained volumetric registration for the early developing brain," *Med Image Anal,* vol. 58, pp. 101540, Dec, 2019.

[4] M. Bossa, E. Zacur, S. Olmos, and I. Alzheimer's Disease Neuroimaging, "Tensor-based morphometry with stationary velocity field diffeomorphic registration: application to ADNI," *Neuroimage,* vol. 51, no. 3, pp. 956-69, Jul 1, 2010.

[5] J. Ashburner, "A fast diffeomorphic image registration algorithm," *Neuroimage,* vol. 38, no. 1, pp. 95-113, Oct 15, 2007.

[6] G. E. Christensen, R. D. Rabbitt, and M. I. Miller, "Deformable templates using large deformation kinematics," *IEEE Trans Image Process,* vol. 5, no. 10, pp. 1435-47, 1996.

[7] M. F. Beg, M. I. Miller, A. Trouvé, and L. Younes, "Computing Large Deformation Metric Mappings via Geodesic Flows of Diffeomorphisms," *International Journal of Computer Vision,* vol. 61, no. 2, pp. 139-157, 2005.

[8] J. Ashburner, and K. J. Friston, "Diffeomorphic registration using geodesic shooting and Gauss-Newton optimisation," *Neuroimage,* vol. 55, no. 3, pp. 954-67, Apr 1, 2011.

[9] M. Kim, G. Wu, P. T. Yap, and D. Shen, "A general fast registration framework by learning deformation-appearance correlation," *IEEE Trans Image Process,* vol. 21, no. 4, pp. 1823-33, Apr, 2012.

[10] S. Tang, Y. Fan, G. Wu, M. Kim, and D. Shen, "RABBIT: rapid alignment of brains by building intermediate templates," *Neuroimage,* vol. 47, no. 4, pp. 1277-87, Oct 1, 2009.

[11] F. L. Bookstein, "Principal warps: thin-plate splines and the decomposition of deformations," *IEEE Transactions on Pattern Analysis and Machine Intelligence,* vol. 11, no. 6, pp. 567-585, 1989.

[12] D. Rueckert, L. I. Sonoda, C. Hayes, D. L. Hill, M. O. Leach, and D. J. Hawkes, "Nonrigid registration using free-form deformations: application to breast MR images" *IEEE Trans Med Imaging,* vol. 18, no. 8, pp. 712-21, Aug, 1999.

[13] Y. Wang, and L. H. Staib, "Physical model-based non-rigid registration incorporating statistical shape information," *Med Image Anal,* vol. 4, no. 1, pp. 7-20, 2000.

[14] B. Rister, M. A. Horowitz, and D. L. Rubin, "Volumetric Image Registration From Invariant Keypoints," *IEEE Trans Image Process,* vol. 26, no. 10, pp. 4900-4910, Oct, 2017.

[15] V. Vishnevskiy, T. Gass, G. Szekely, C. Tanner, and O. Goksel, "Isotropic Total Variation Regularization of Displacements in Parametric Image Registration," *IEEE Trans Med Imaging,* vol. 36, no. 2, pp. 385-395, Feb, 2017.

[16] T. Vercauteren, X. Pennec, A. Perchant, and N. Ayache, "Diffeomorphic Demons: Efficient non-parametric image registration," *Neuroimage*, vol. 45, no. 1, pp. 61–72, 2009.

[17] Avants, B. B., Epstein, C. L., Grossman, M., and Gee, J. C. "Symmetric diffeomorphic image registration with cross-correlation: Evaluating automated labeling of elderly and neurodegenerative brain". *Med Image Anal*, vol.12, no. 1, pp. 26–41, 2008.